



Fabrication of a sensitive and selective electrochemical sensing platform based on poly-L-leucine modified sensor for enhanced voltammetric determination of Riboflavin

Amrutha Balliamada Monnappa^{1,2} · Jamballi Gangadharappa Gowda Manjunatha¹ · Aarti Sripathi Bhatt² · Pushpanjali Pemmatte Ananda¹

Received: 15 June 2020 / Accepted: 17 August 2020 / Published online: 24 August 2020
© Springer Science+Business Media, LLC, part of Springer Nature 2020

Abstract

Riboflavin (RB) plays a pivotal role in cell growth and various biochemical reactions in the human body. Low level of RB leads to various health related issues and hence it is imperative to develop a sensitive and selective method for determination of RB. Electrochemical property of RB at poly-L-leucine modified carbon paste electrode (PLMCPE) was examined by cyclic voltammetry (CV) and differential pulse voltammetry (DPV) in 0.2 M phosphate buffer solution (PBS) of an optimum pH of 6.5. Favourable interaction between L-leucine (L-leu) film and RB enhance the redox current response in comparison with bare carbon paste electrode (BCPE). The process at the exterior of the electrode was noticed to be reversible and diffusion controlled in the potential window of -0.8 to 0 V/s. The surface characterisation of fabricated PLMCPE was accomplished by Field emission scanning electron microscopy (FE-SEM) and Electronic impedance spectroscopy (EIS). Parameters like electrochemical active surface area of the sensor, number of electrons transferred, surface concentration and heterogeneous rate constant were calculated. Under optimised condition DPV and CV divulge a notable linear relationship in between the oxidation peak current of RB and concentration of RB with a detection limit (LOD) of 3.4×10^{-8} M and 4.02×10^{-8} M respectively. Various interferant metal ions were used to investigate the interference effect and was found that the method is compelling, selective and sensitive towards detection of RB. The performance of PLMCPE was triumphantly tested for the detection of RB in vitamin capsules by DPV and the excellent recovery proves that the proposed method can be constructively used for real sample analysis.

Keywords Carbon paste electrode · Poly-L-leucine · Modified sensor · Riboflavin · Vanillin

Introduction

RB or Vitamin B₂ is a water-soluble vitamin which plays a crucial role in various biochemical reactions of human body like haemoglobin synthesis, drugs and xenobiotics, hydrogen carrier in the course of carbohydrate, protein and lipid metabolism [1]. It is a vital component of flavoenzymes which displays a significant role in the flavoprotein enzyme

reaction and plays a pivotal role as component of electron transport system in tissue oxidation. It cannot be synthesized in human body and therefore intake of dietary supplements like organ meat, fish, milk, certain fruits and green vegetables are sources of high concentration of RB. RB deprivation in human body arises within a few days after depletion in dietary supplement intake. Primary deficiency of RB has massive implication on the efficacy of other vitamins since this parent compound is directly linked to metabolism of fat, cobalamin, folic acid, niacin, vitamin K, vitamin D and pyridoxine [2]. Inadequate amount of RB concentration in human body can lead to obvious health issues like beriberi, hypochromic anaemia, congenital disabilities during pregnancy, oxidative damage of tissues and depletion in hematologic response. RB depletion also increases the risk of cancer [3–5].

✉ Jamballi Gangadharappa Gowda Manjunatha
manju1853@gmail.com

¹ Department of Chemistry, FMKMC College, Madikeri, Constituent College of Mangalore University, Mangalore, Karnataka, India

² Department of Chemistry, N.M.A.M. Institute of Technology, (Visvesvaraya Technological University, Belgavi) Nitte, Udupi District, Karnataka 574110, India

Consequently, it is of paramount importance to develop an effective, highly sensitive, reliable and selective method for the quantitative analysis of RB. Numerous sophisticated analytical methods like high performance liquid chromatography (HPLC) [6], spectrophotometry [7], fluorescence [8], Liquid Chromatography with mass spectrometry (LC–MS) [9] were employed for the quantitative and qualitative determination of RB. But these methods are tedious, time consuming, expensive and they have complicated sample preparing procedure. Owing to their modest, sensitive, reasonable cost of instrumentation and rapid response time electrochemical methods have garnered phenomenal interest for the sensitive analysis of bioactive moieties [10, 11]. Several electrochemical sensors like graphene paste electrode, modified glassy carbon electrode, nano carbon composite electrode, carbon paste electrode etc. [12–15] are fabricated for the voltammetric determination of RB, where all these fabricated sensors have their own individual advantages and drawbacks [16–21].

Carbon paste electrodes (CPE) are extensively used electrode material for the fabrication of various biosensors and electrochemical sensors because of their low cost, porous renewable surface, low residual current in wide potential window, acceptable robustness and easy modification of the electrode surface [22–29]. Electro polymerisation method proves to be a reliable tool for the detection of various electroactive species since the electro polymer modified electrode forms a homogeneous deposition of polymer layer with strong adherence power at the carbon paste electrode [30]. These electrode displays specific enhanced sensitivity, minimum possibility to be influenced by surface fouling and are accomplished enough to provide low detection limit. In electrochemical method the application of Amino acid as a modifying material has attracted researchers due to their unique advantage of biocompatibility over their counterparts. Due to the large concentration of reactive groups on the surface highly stable sensitive electrochemical response will be displayed [31–33]. In this paper we have adopted a modest, swift and convenient poly-L-leucine modified carbon paste electrode for the mechanistic investigation of RB by CV and DPV methods.

Methods and materials

Instrumentation

Electrochemical experiments were conducted by using electrochemical work station CHI-6038E model (CH Instrument-6038 electrochemical workstation-USA) at ambient temperature. The electrochemical cell was assembled with ideal tri electrode system equipped with BCPE and PLM-CPE as working electrodes, KCl saturated calomel and

platinum counter electrode. FE-SEM was performed using the instrument working at 5.00 kV from DST-PURSE Laboratory, Mangalore University.

Chemicals and solutions

Carbon powder, Silicone oil and Potassium chloride were purchased from Nice Chemicals (Cochin) India. Mono sodium dihydrogen phosphate, disodium hydrogen phosphate and L-leucine were procured from Himedia chemicals (India), RB and VN were obtained from Molychem laboratory, India. Double distilled water was utilised for dissolving the essential amount of solute to get 25×10^{-4} M RB and VN stock solution. 25 mM stock solution of L-leu was prepared by suspending the required amount of solute in double distilled water. The 0.2 M Phosphate buffer solution (PBS) of different pH values were prepared by inter mixing the suitable quantity of 0.2 M Na_2HPO_4 and 0.2 M NaH_2PO_4 . Real sample solution was prepared by weighing appropriate quantity of commercially available RB samples and was dissolved in an amber coloured volumetric flask with double distilled water to get a standard solution of 25×10^{-4} M strength.

Preparation of BCPE and PLMCPPE

BCPE was developed by mixing 70% graphite powder and 30% silicon oil as a binder in an agate mortar. The mixture was homogenised by grinding it for 20 min into a fine paste with the help of a pestle. A small portion of mixture was tightly packed into the Teflon tube of 3 mm internal diameter which was rubbed on the tissue paper to get a uniform smooth surface. The electrical contact was delivered by embedding a copper wire into the Teflon tube from opposite direction. Polymerisation of L-leu onto CPE was carried out by subsequently running 10 potential cycles on BCPE between -1.5 to 3.0 V in an aqueous PBS containing 1×10^{-3} M L-leu monomer.

Results and discussions

Electrochemical polymerisation of L-leu

Figure 1a displays the cyclic voltammograms of poly-L-leu film deposition on the CPE at a scan rate of 0.1 V/s in PBS of pH 6.5 containing 1×10^{-3} M L-leu monomer solution. During the forward scan L-leu monomer oxidation peak was detected at 0.340 V corresponding to the formation of oxidised L-leu and during the reverse scan the reduction peak was detected at -0.196 V which corresponds to reduced L-leu. The advance of steadily increasing redox waves and the enhancement in both oxidation and reduction peak current

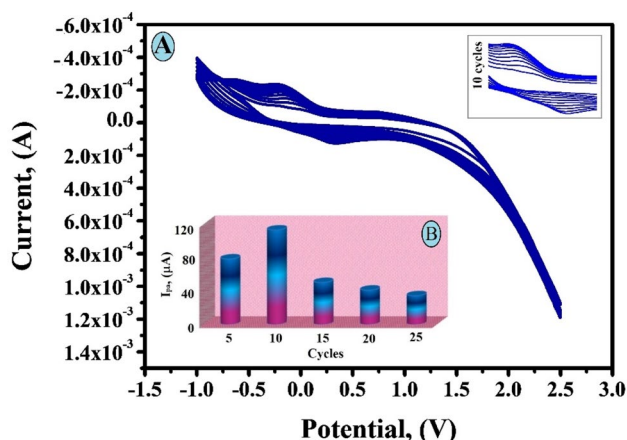
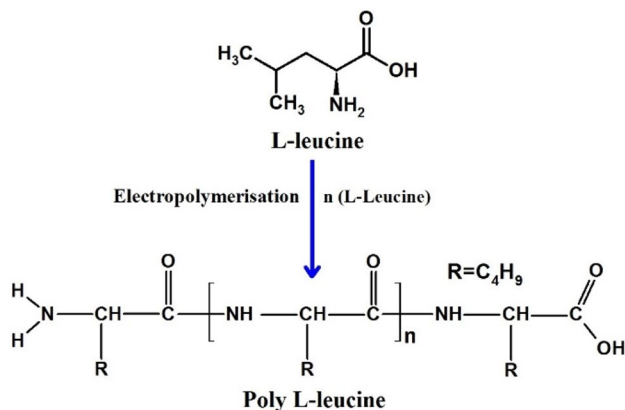


Fig. 1 (a) Cyclic voltammogram of electrochemical polymerisation of 1×10^{-3} M L-leu in 0.2 M PBS of pH 6.5 within the potential window -1.5 V to 3.0 V at a scan rate 0.1 V/s. (b) Plot of the oxidative peak current of 1×10^{-3} M L-leu versus the number of polymerization cycles

with each potential cycle specifies the deposition of bioactive polymer film on the surface of CPE [34–36]. The probable mechanism is represented in Scheme 1. After modification PLMCPE was rinsed with double distilled water and utilised for subsequent determinations.

The electrocatalytic activity of the fabricated electrode depends on the thickness of the polymer film. Poly-L-leu film of various thickness was obtained by altering the number of scan cycles from 5 to 25. Figure 1b in the inset displays the peak current augmented up to the 10th cycle and after that the peak current diminished, which may be ascribed to the actuality that till 10th cycle is reached complete surface coverage of CPE takes place which results in the surge of active sites and after that electron transferring nature of L-leu gets depleted and as a ramification of that the peak current gets diminished. Hence, the number of scan cycles for electro polymerisation of L-leu was fixed to 10 cycles.



Scheme 1 Probable mechanism of L-leucine polymerization

Electrochemical active surface area

The electrochemical interaction between the surface of the PLMCPE and the target analyte was deliberated by CV using 1 mM $K_4[Fe(CN)_6]$ as a redox probe containing 0.1 M KCl as supportive electrolyte at a sweep rate of 0.1 V/s. From the CV displayed in Fig. 2 it is obvious that PLMCPE (curve a) shows remarkably magnified anodic peak current ($I_{pa} = 26.33 \mu A$) in comparison with that of BCPE which portrays a diminished I_{pa} ($10.04 \mu A$). This enhancement in peak current of PLMCPE is credited to the fact that there are additional electrochemical active sites due to the development of a thin film of poly- L-leu on the exterior of the electrode. PLMCPE shows ΔE_p (difference between E_{pa} and E_{pc}) value of 0.115 V which is less than that of BCPE which displays a ΔE_p value of 0.249 V, suggesting that the polymer film on the electrode surface facilitates faster electron transfer [37–39].

Randles–Sevcik equation is applied to calculate the electrochemical surface area of BCPE and PLMCPE;

$$I_{pa} = 2.69 \times 10^5 n^3/2 A C_0 D^{1/2} \nu^{1/2} \tag{1}$$

where I_{pa} represents anodic peak current, n indicates number of electrons exchanged, C_0 represents strength of electroactive species, D specifies diffusion coefficient, ν is the scan rate. The electrochemical active surface area ‘A’ of PLMCPE and BCPE was found to be 0.036 cm² and 0.014 cm² respectively. The active surface area of PLMCPE is almost twice greater than that of BCPE which certifies it to be a robust proof for the fruitful and constructive modification of CPE by a polymer film of poly-L-leu.

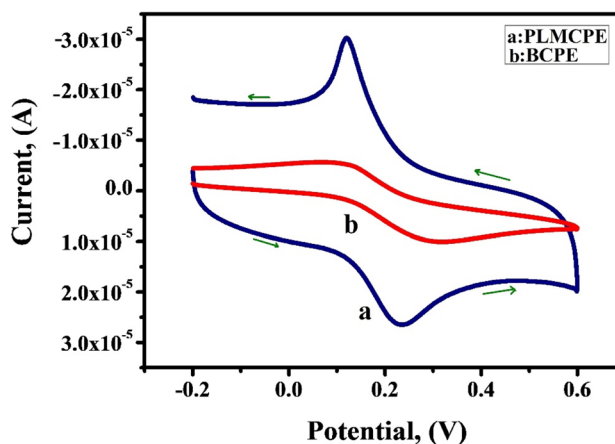


Fig. 2 Cyclic voltammograms of 1 mM $K_4[Fe(CN)_6]$ at BCPE and PLMCPE in 0.1 M KCl at the scan rate of 0.1 V/s

Surface morphological study by FE-SEM and EIS

Figure 3 reveals the surface morphology of BCPE (Fig. 3a) and PLMCPE (Fig. 3b) using FE-SEM. BCPE displays a rough dense surface with flakes like structure of Graphite and on modification PLMCPE displays a lamellar deposition of polymer film over the graphite flakes. It shows that poly-L-leucine film has good porosity which enhances the active surface area of the electrode and thereby promoting the efficiency of electrode functionalisation.

EIS is an effectual method extensively used as a standard characterisation technique of electrode surface since it is highly surface sensitive [40]. Experimental outcome of EIS measurement are plotted in a Nyquist diagram which represent the imaginary part of impedance measurement along y-axis and real part along x-axis. Redox couple containing 1 mM $K_4[Fe(CN)_6]$ in 0.1 M KCl solution was used as a standard analyte. The diameter of the semi-circular portion of the Nyquist plot is equal to the electron transfer kinetics controlled by the charge transfer resistance (R_{ct}) for the concerned electrochemical reaction. Figure 4 displays the Nyquist plot for BCPE (curve a) and PLMCPE (curve b). From the plot it is clear that PLMCPE displays smaller semicircle in comparison with BCPE which indicates the synergistic effect of conductivity in promoting the electron transfer rate at interface of PLMCPE and the redox probe [41, 42]. This indicates that poly-L-leucine film can act as an effective electron conducting pathway between the electrode surface and analyte.

Absorbance studies of RB

Since UV–Visible (Ultraviolet visible) spectrum is a simple way to analyse coloured species it is expansively used to study the light absorption and light intensity properties by

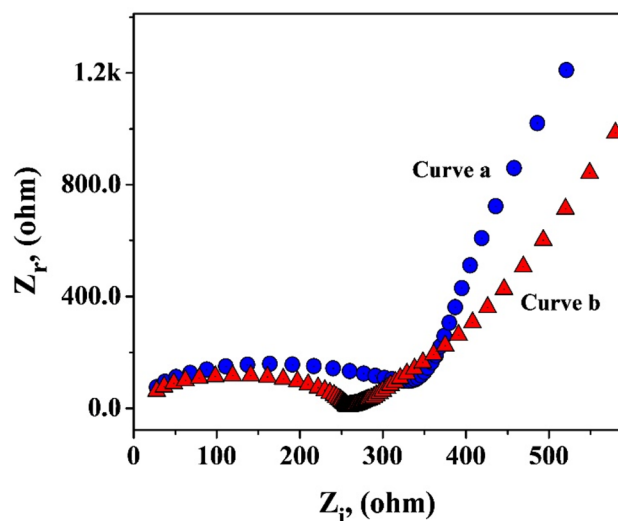


Fig. 4 Nyquist diagrams of EIS of BCPE (curve a) and PLMCPE (curve b)

dyes. The absorbance spectra of RB were accomplished in a cuvette containing 0.2 M PBS of pH 6.5 where the wavelength range spanned from 150 to 600 nm. Figure 5 displays three absorbance peaks where maximum absorbance was observed at 260 nm and this wavelength is of interest for the quantitation of RB [43].

Influence of pH

The pH of the buffer has a remarkable role in determining the mechanism of electrochemical behaviour of RB at PLMCPE. By optimising the pH of a solution, it is feasible to secure a sharper response escorted with elevated sensitivity. Hence, the impact of pH on the redox potential and redox current was estimated in 0.2 M PBS

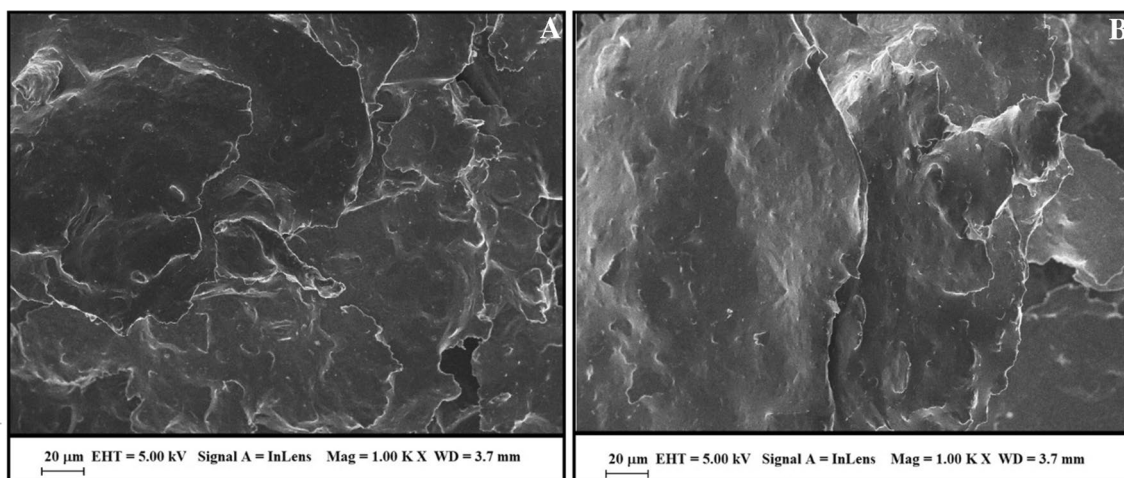


Fig. 3 FESEM images of BCPE (a) and PLMCPE (b)

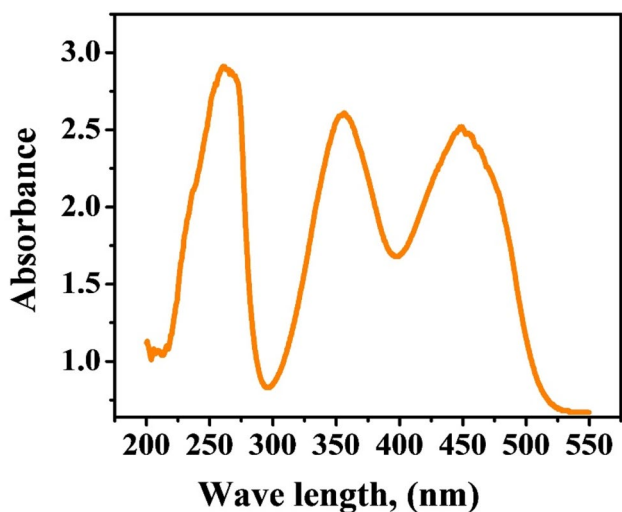


Fig. 5 UV-Vis spectrum of RB

of different pH spanning from 5.5 to 8 which was investigated by CV technique. Figure 6a represents the cyclic Voltammogram obtained on varying the pH from 5.5 to 8.0. The results obtained from CV portrays that ΔI_p value increases with increase of pH, reaches a maximum at 6.5

and thereafter the decline is attributed to the degradation of RB at higher pH in ambient light [44]. The plot of I_{pa} vs pH (Fig. 6b) exhibits an augmented peak current at pH 6.5 and hence this pH was appraised to be optimum for further determinations. The rate of electrochemical redox reaction has a direct impact on the magnitude of peak current. The linear relationship between E_{pa} and pH displayed in Fig. 6c is expressed with a linear regression equation $E_{pa} \text{ (V)} = 0.07823 - 0.058 \text{ pH}$ with $R^2 = 0.9893$. From the Fig. 6c it is obvious that the peak potential moves to less positive side with the escalation of pH. The slope of 0.058 V which is in close approximate with the Nernstian slope specifies that the number of protons and electrons taking part is in the ratio 1:1 where two protons and two electrons are involved according to the available literature on oxidation of RB. The probable mechanism is represented in Scheme 2 [45]. Number of electrons transferred can be calculated by the equation [46]:

$$\alpha n = 1.857 RT / (E_{pa} - E_{pa/2}) F \tag{2}$$

where α is the charge transfer coefficient, E_{pa} is the anodic peak potential, $E_{pa/2}$ is the half wave potential for anodic peak and rest of the values have their own significance. The

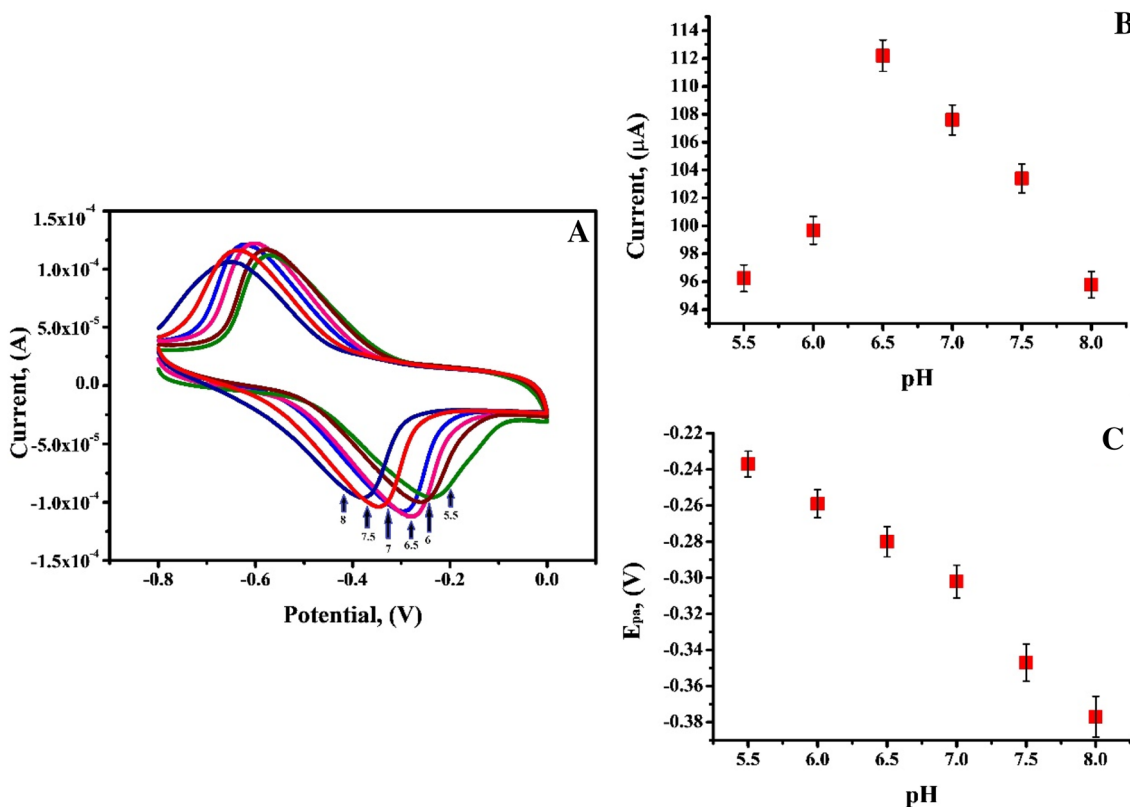
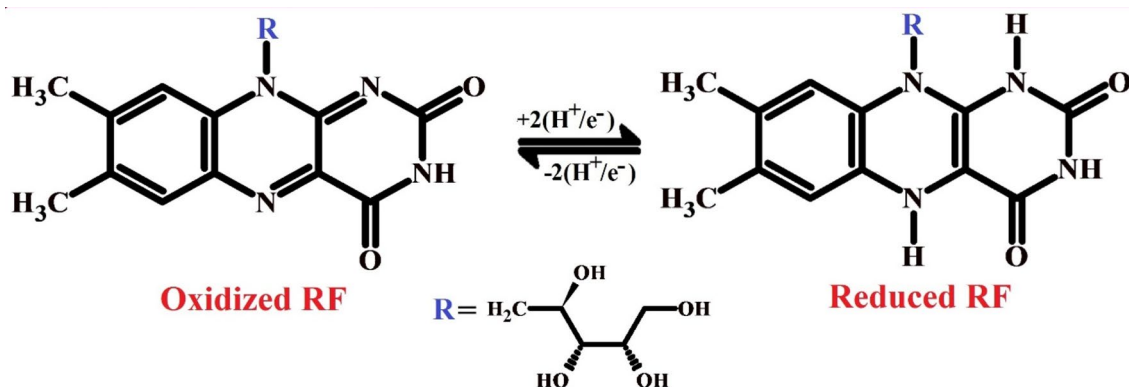


Fig. 6 a Cyclic Voltammogram obtained for influence of supporting electrolyte of 0.2 M PBS on 1×10^{-4} M RB at PLMCPE with a scan rate of 0.1 V/s. b Plot of I_{pa} versus pH at PLMCPE with error bars (N=3). C Plot of E_{pa} Vs pH at PLMCPE with error bars (N=3)



Scheme 2 Probable redox mechanism of RB at PLMCPE

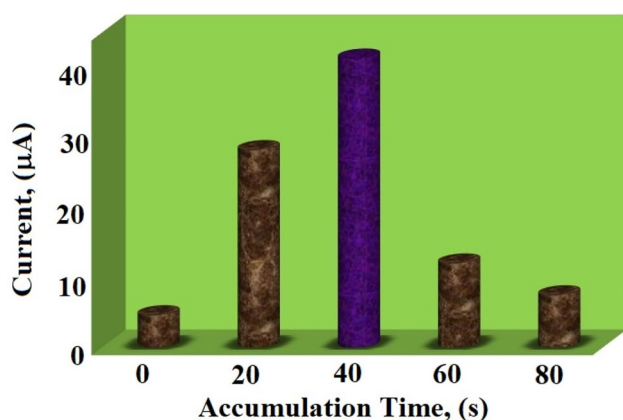


Fig. 7 Plot of anodic peak current of 1×10^{-4} M RB at PLMCPE as a function of accumulation time

number of electrons exchanged was found to be 1.67 which was appraised to be equal to two [47].

Accumulation time

The magnitude of the peak current is directly dependent on the amount of electroactive species present in the vicinity of electrode surface. Figure 7 represents the graph of anodic peak current as a function of accumulation time. Analysis was performed in the interval of zero to eighty seconds in 0.2 M PBS of pH 6.5 containing 1×10^{-4} M RB at a scan rate of 0.1 V/s. The experimental results portray that from zero to forty seconds the peak current surges linearly with the accumulation time which can be ascribed to the rapid adsorption of RB on the surface of PLMCPE. Further, after forty seconds the peak current exhibits a steady decline which is due to the saturation of RB at the electrode surface [48, 49]. Hence, forty seconds was considered as the optimum accumulation time interval for subsequent determinations.

Electrocatalytic behaviour of RB at PLMCPE

The comparative study of the electrocatalytic activity of BCPE and PLMCPE was done by CV and DPV technique. Figure 8a demonstrated the cyclic voltammograms of RB at PLMCPE (curve a) and BCPE (curve c) under optimum conditions. The voltammogram obtained for the detection of RB at BCPE portrays dimly readable peaks with anodic peak potential of -0.407 V and cathodic peak potential of -0.499 V. On the contrary PLMCPE yields sharp redox peaks with enhanced current sensitivity with anodic peak potential of -0.280 V and cathodic peak potential of -0.602 V. The enhanced current sensitivity ($I_{pa} = 112.2$ μA) obtained at PLMCPE is due to a faster rate of electron transfer during the redox reaction of RB [50, 51]. The voltammogram (curve b) obtained in Fig. 8a exhibits the blank response of PLMCPE in 0.2 M PBS of pH 6.5 at a scan rate of 0.1 V/s. Figure 8b establishes the DPV for electrochemical behaviour of RB at PLMCPE (curve a) and BCPE (curve b) under optimum conditions. Augmented current sensitivity is observed for PLMCPE in comparison with BCPE. From the enhanced redox peak current obtained it is apparent that the surface of BCPE is modified by a polymer film of L-leu, as a result of which a phenomenal increase in the affinity of electrode for the oxidation of RB was observe.

Linearity, detection limit and quantification studies through CV and DPV

CV and DPV methods were used to study the correlation between the variation of RB concentration and the peak current under optimised experimental condition. Figure 9a displays the differential pulse voltammograms of RB at PLMCPE within the concentration range of 2 μM to 50 μM where the peak current amplifies with the rise in concentration of RB. Linearity is observed in the plot of oxidation peak current of RB and concentration of RB (Fig. 9b), but

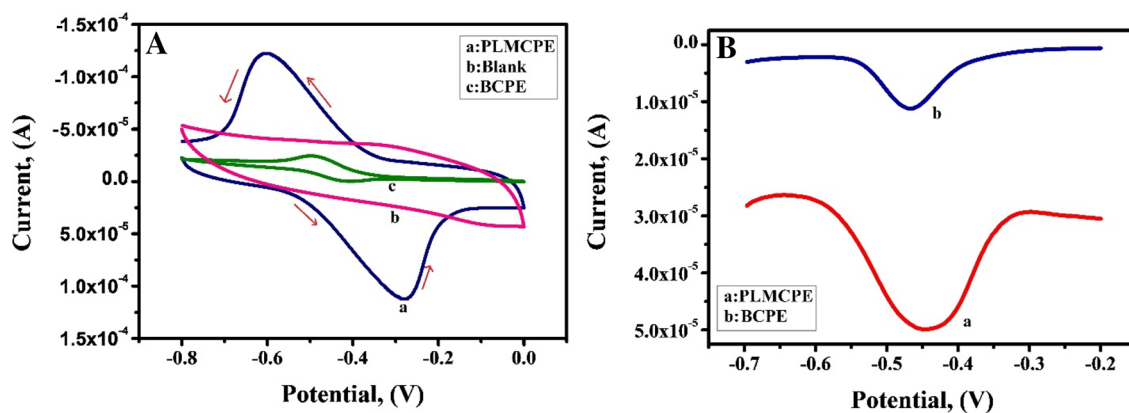


Fig. 8 a CV response of 1×10^{-4} M RB at PLMCPE (curve a), BCPE (curve c) and Blank solution (curve b) in 0.2 M PBS of pH 6.5 at a scan rate of 0.1 V/s. b DPV response of 1×10^{-4} M RB at PLMCPE (curve a) and at BCPE (curve b) under optimum condition

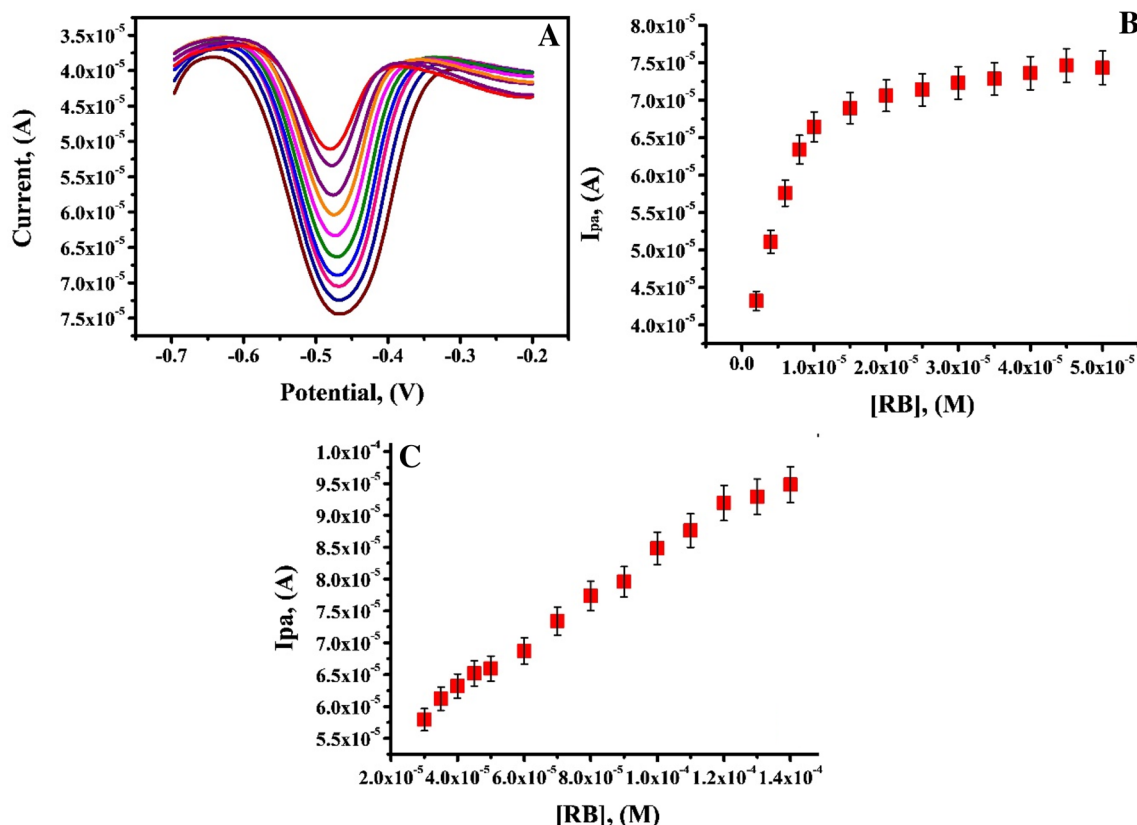


Fig. 9 a Differential pulse voltammograms for variation of peak current with the concentrations of RB at PLMCPE in 0.2 M PBS of pH 6.5. b The plot of anodic peak current against the concentration of RB (2 μ M to 50 μ M) from DPV with error bars (N=3). c Calibra-

tion plot between anodic peak current values of RB and the altered concentrations of RB in the range 2 μ M to 140 μ M by CV with error bars (N=3)

we considered the first linear range from 2 to 10 μ M with a linear regression equation, I_{pa} (μ A) = $3.87 \times 10^{-5} + 2.938$ [RB] (M) ($R^2 = 0.9901$). From the obtained analytical data LOD and LOQ was calculated to be 3.4×10^{-8} M and 11.4×10^{-8} M respectively.

(LOD = $3S/N$ and LOQ = $10 S/N$; S is the Standard deviation of 0.2 M PBS; N is the slope of calibration plot) [52–54].

Figure 9c demonstrates the linear calibration plot obtained for anodic peak current of RB versus concentration

variation of RB in the range 2 μM to 140 μM by CV technique at PLMCPE under optimum condition. From the plot it is noteworthy that with the surge in concentration of RB the peak current intensified linearly and the first linear range was considered from 2 to 25 μM . The linearity is expressed by the equation, $I_{\text{pa}} (\mu\text{A}) = 8.29 \times 10^{-6} + 1.9572 [\text{RB}] (\text{M})$ ($R^2 = 0.9862$). LOD and LOQ from the CV technique was found to be $4.02 \times 10^{-8} \text{ M}$ and $13.42 \times 10^{-8} \text{ M}$ respectively. Table 1 shows the comparison of LOD and LOQ values at PLMCPE by DPV and CV methods with other works reported in the literature. The comparative study of few modified sensors reveals that PLMCPE is in par with other electrodes in its electrocatalytic activity towards the detection of RB and proves to be more advantageous since the fabricated sensor is of low cost, easy fabrication procedure and above all its biocompatible.

Impact of scan rate

Evaluation of cyclic voltammogram of RB at varied scan rate proffered information regarding the dependence of anodic peak current with scan rate and nature of electrode process taking place at the electrode surface. From the cyclic voltammograms (Fig. 10a) obtained for investigation of RB in 0.2 M PBS of pH 6.5, it is clear that the peak current is proportional to scan rate indicating the direct transfer of electron between the fabricated sensor and the analyte. With the intensification of scan rate from 0.050 to 0.3 V/s the anodic peak potential is found to shift towards more positive side and cathodic peak potential shifts towards more negative side with a considerable change in ΔE_p value indicating that the redox action of RB is quasi reversible. Plot of I_{pa} versus square root of scan rate (Fig. 10b) suggested the process is diffusion controlled since it exhibits linearity with a correlation coefficient 0.9989 and linear regression equation, $I_{\text{pa}} (\mu\text{A}) = -55.28 + 532.46 v^{1/2} (\text{V/s})$.

Further plot of peak potential versus log of scan rate (Fig. 10c) was deliberated which exhibited a good linear relationship with the regression equation: $E_{\text{pa}} = 0.0129 + 0.2550 \log v$; $R^2 = 0.9922$.

The heterogeneous rate constant (k_0) for the rate of transfer of electrons in between the interface of the electrode surface and analyte is calculated to be $0.32 \times 10^{-2} \text{ s}^{-1}$ by using Eq. 3 [58]:

$$\Delta E_p = E_{\text{pa}} - E_{\text{pa}/2} = 201.39 [\log(v/k_0)] - 301.78 \quad (3)$$

E_{pa} corresponds to the anodic peak potential, $E_{\text{pa}/2}$ represents the potential where the current is half the peak value, k_0 symbolises the rate constant and v is the scan rate in V/s.

The surface concentration (Γ) of the electroactive species was calculated to be 8.3 nmol/cm^2 by applying the equation:

$$Q = nFA\Gamma \quad (4)$$

where Q denotes the integrated charge from the area of cyclic voltammetry peak, n indicates the number of electrons taking part in the reaction, F is Faradays constant, A is the modified electrode surface area [59, 60].

Selectivity of PLMCPE for the sensitive determination of RB in presence of VN by CV and DPV method

VN is one of the most expansively used food flavouring agent. It is widely used in pharmaceuticals, cream products and beverage industries. Since both these moieties play noteworthy role in human system, the meticulous sensing proficiency of PLMCPE was evaluated by taking $1 \times 10^{-4} \text{ M}$ RB and $1 \times 10^{-4} \text{ M}$ VN in 0.2 M PBS of pH 6.5 at a scan rate of 0.1 V/s. Figure 11a exhibits the CV for the concurrent determination of RB and VN at PLMCPE (curve a) and BCPE (curve b) where BCPE exhibits diminished current response. On the contrasting

Table 1 Comparison of the LOD values of PLMCPE with previously reported sensor for voltammetric determination of RB

Working electrode	Method	Linear range (μM)	LOD (M)	References
SnO ₂ /RGO nano composite modified glassy carbon electrode	SWV	0.1–150	34×10^{-9}	[55]
MnO ₂ modified carbon paste electrode	DPV	0.02–9	15×10^{-9}	[28]
Homoadenine single-stranded DNA/molybdenum disulphide graphene nanocomposite modified gold electrode	DPV	0.025–2.25	20×10^{-9}	[10]
Zeolite modified carbon paste electrode	CV	1.7–34	0.71×10^{-6}	[1]
Palladium–Copper nano particles modified porous carbon electrode	DPV	0.02–9	7.6×10^{-12}	[56]
DNA functionalised pencil graphite electrode	DPV	1–186	0.9×10^{-6}	[57]
Cr-SnO ₂ nano particles modified glassy carbon electrode	DPV		1.47×10^{-7}	[11]
Poly leucine modified carbon paste electrode	DPV	2–50	3.4×10^{-8}	Present work
	CV	2–140	4.02×10^{-8}	

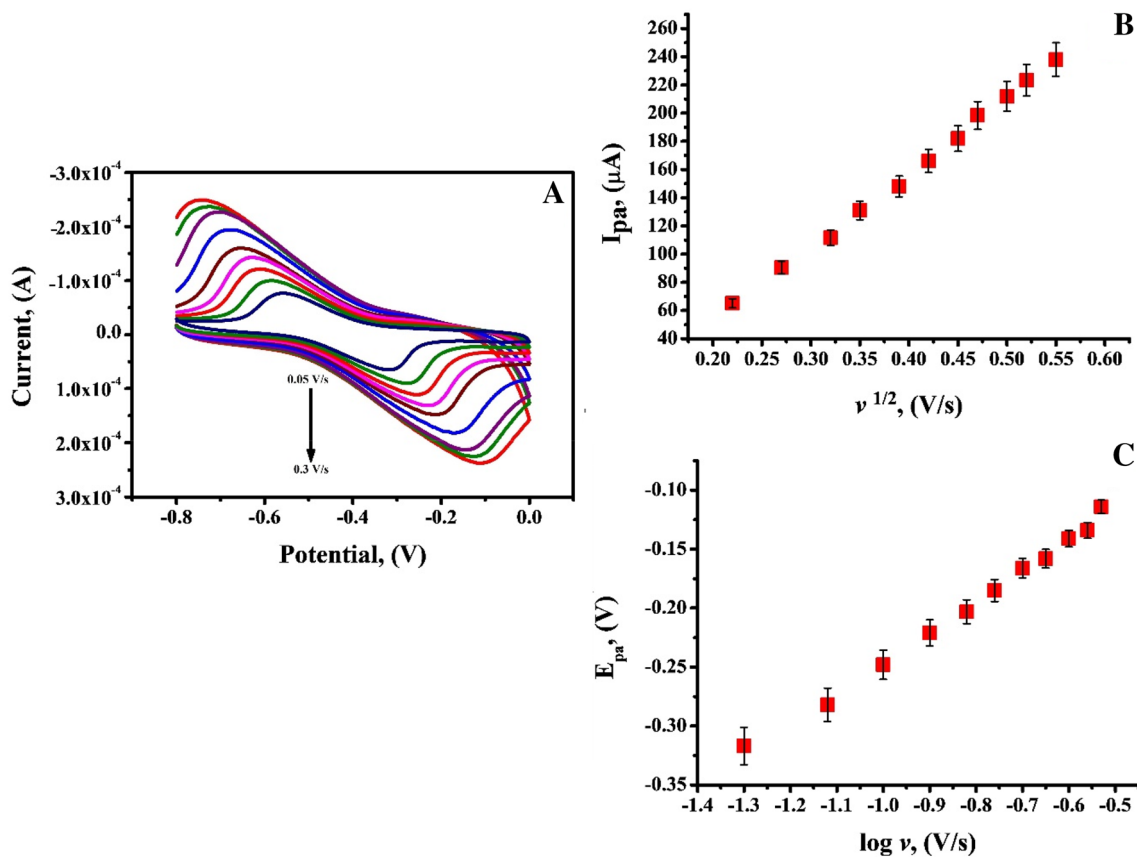


Fig. 10 a Cyclic voltammogram of 1×10^{-4} M RB in 0.2 M PBS of pH 6.5 at PLMCPE at various scan rates (0.05 V/s to 0.3 V/s). b Plot of I_{pa} (μ A) vs. square root of scan rate ($v^{1/2}$) with error bars (N=5). c Plot of E_{pa} (V) vs log of scan rate ($\log v$) with error bars (N=5)

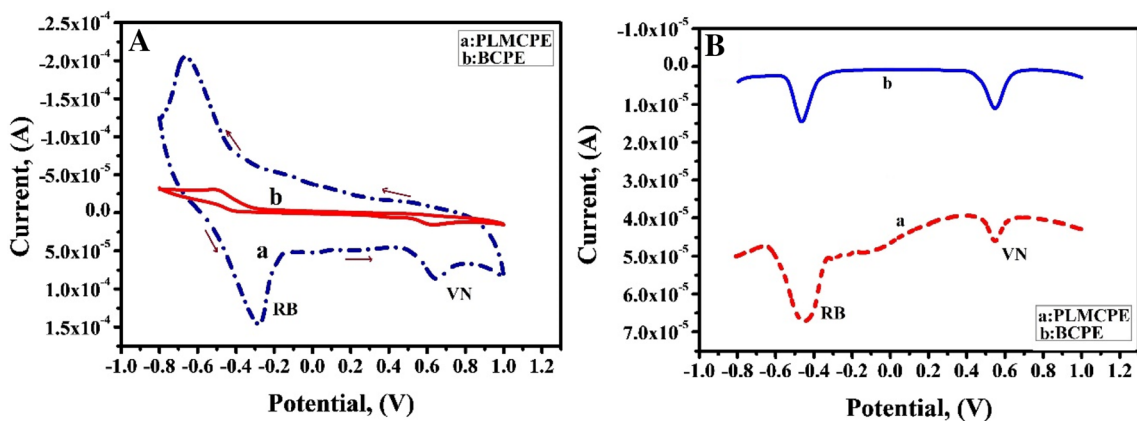


Fig. 11 a CV response for simultaneous determination of RB and VN (1×10^{-4} M) at PLMCPE (curve a) and BCPE (curve b) b DPV response for simultaneous determination of RB and VN (1×10^{-4} M)

at PLMCPE (curve a) and BCPE (curve b) in 0.2 M PBS of pH 6.5 at a scan rate of 0.1 V/s

side, PLMCPE displays two well separated peaks for RB and VN with enhanced current sensitivity at a potential of -0.286 V and 0.650 V respectively. Figure 11b displays the DPV diagram for concurrent determination of RB in presence VN at PLMCPE (curve a) and BCPE (curve b).

In comparison with BCPE, the modified electrode exhibits enhanced current sensitivity with two peaks separated by a wide potential. Hence, it is clear that the electrocatalytic activity of PLMCPE towards RB remains unruffled even in the presence of VN.

Interference studies

The selectivity of the fabricated sensor towards the detection of RB along with various potentially interfering species were analysed under optimum condition. Hand-picked samples of certain anions and cations present in the body or the food we take were chosen. The interference analysis was performed by taking metal ions like Fe^{3+} , K^+ , Mg^{2+} , Na^+ , Ca^{2+} , Zn^{2+} and Cl^- ion. The existence of these ions in the similar concentration range as of RB do not alter the peak current and peak potential of RB which withstands the fact that PLMCPE can be employed for selective determination of RB [61].

Examination of reproducibility, repeatability and stability

Reproducibility, repeatability and stability are the parameters used to gauge the sensing performance of the modified sensor under the optimum condition. A series of five modified electrodes were fabricated in the same procedure and CV response of 1×10^{-4} M RB was recorded consecutively for five trials. The relative standard deviation (RSD) of 4.78 was obtained which indicates excellent reproducibility of PLMCPE. The repeatability of the PLMCPE was studied by running five successive CV cycles and the outcome provides excellent repeatability with an RSD of 4.64. The stability of the modified electrode was deliberated by running 30 consecutive cycles and it was found that 94.8% of initial current is retained even after running 30 cycles.

Percentage degradation = $\frac{I_{pn}}{I_{p1}} \times 100$ where I_{pn} is the peak current at nth cycle and I_{p1} is the peak current at the first cycle [62, 63].

Application to pharmaceutical sample

PLMCPE was used for the analysis of RB in pharmaceutical samples to prove its viability in real sample analysis. Standard addition method of the prepared sample solution was incorporated under optimised experimental condition and the results are tabulated in Table 2. The working electrode demonstrates a recovery in the range of 96.02 to 100.21% for

Table 2 Estimation of RB in pharmaceutical sample

Sample	Added (μM)	Found (μM)	Recovery (%)
B-Complex capsule	4.35	4.19	96.32
	9.45	9.47	100.21
	13.56	13.02	96.02
	17.92	17.32	96.66
	22.34	21.77	97.45

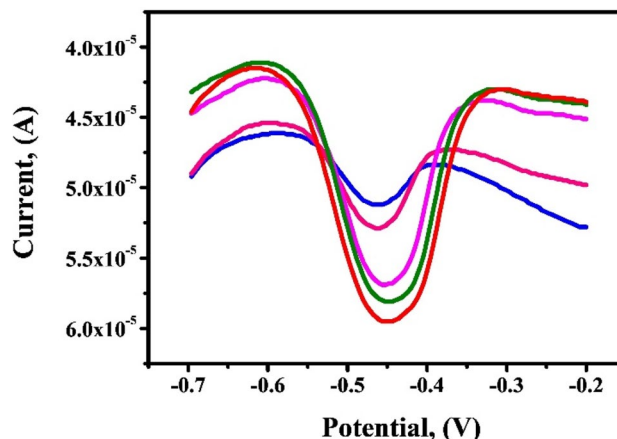


Fig. 12 DPV obtained for variation of peak current with variation of concentration of RB at PLMCPE under optimized experimental parameters

the pharmaceutical sample. The DPV curves for real sample analysis are portrayed in Fig. 12. The data obtained for the analytical sample analysis manifest the fact that fabricated sensor is distinctly reliable with thorough sensing performance and can be successfully employed for the analysis of RB in pharmaceutical samples.

Conclusion

A stable and well-defined polymer film of L-leu was formed on CPE by cycling the electrode potential continuously in the potential window of -1.5 V to 3.0 V in 0.2 M PBS of pH 6.5 containing 1×10^{-3} M L-leu. The PLMCPE displays enhanced current sensitivity and selectivity towards the detection of RB in both real and commercially available samples by CV and DPV methods. The surface topography was studied by FESEM, EIS and surface area of PLMCPE and BCPE was determined by using redox probe $\text{K}_4[\text{Fe}(\text{CN})_6]$ which was calculated to be 0.036 cm^2 and 0.014 cm^2 respectively. The voltammetric response for the redox action of RB was found to be maximum at pH 6.5 which demonstrates that the process is diffusion controlled and comprises two electrons and two protons. By using the fabricated electrode, RB concentration as low as 3.4×10^{-8} M and 4.02×10^{-8} M can be determined with DPV and CV methods. The proposed method shows excellent sensitivity and selectivity for interference studies of RB with other metal ions and simultaneous studies.

Compliance with ethical standards

Conflict of interest No conflict of interest with any organization, reviewers and authors for this work.

References

- E.A. Nezamzadeh, P.J. Pouladsaz, *J. Ind. Eng. Chem.* **20**(4), 2146–2152 (2013)
- J.T. Pinto, J. Zempleni, *Adv. Nutr.* **7**(5), 973–975 (2016)
- H.J. Powers, *Am. J. Clin. Nutr.* **77**(6), 1352–1360 (2003)
- L. McDowell, *Vitamin History the Early Years*, 1st edn. (Sarasota Publishers, Sarasota, 1939), p. 54
- C.N. Cioates, *J. Electrochem. Soc.* **167**, 084514 (2020)
- B.J. Petteys, E.L. Frank, *Clin. Chim. Acta.* **412**, 38–43 (2011)
- R. Bartzatt, T. Wol, *Int. Sch. Res. Not.* **2014**, 1–7 (2014)
- K.F. Michaelsen, L.M. Neufeld, A.M. Prentice, 11th edition (Nestle Nutrition Institute, 2012), pp. 1–3
- Z. Nazanin, Z.C. Babur, F.S. Pullen, M.J. Snowden, J. Tetteh, *Food Chem.* **135**(4), 2743–2749 (2012)
- H. Feng, Z. Huang, X. Lou, J. Li, G. Hui, *Food Anal. Methods* **10**, 407–418 (2017)
- G. Hui, J. Zhang, J. Li, L. Zheng, *Food Chem.* **197**, 1168–1176 (2016)
- Y. Wang, Q. Zhuang, Y. Ni, *J. Electroanal. Chem.* **736**, 47–54 (2014)
- N. Lavanya, S. Radhakrishnan, C. Sekar, M. Navaneethan, Y. Hayakawa, *Analyst* **138**, 2061–2067 (2013)
- L.C. Gribat, J.T. Babauta, H. Beyenal, N.A. Wall, *J. Electroanal. Chem.* **798**, 42–50 (2017)
- M.M. Motaghi, H. Beitollahi, S. Tajik, R. Hosseinzade, *Int. J. Electrochem. Sci.* **11**, 7849–7860 (2016)
- Z.S. Azad, M.A. Taher, S. Cheraghi, H.K. Maleh, *J. Food Meas. Charact.* **13**, 1781–1787 (2019)
- M. Bijad, H.K. Maleh, M. Farsi, S.A. Shahidi, *J. Food Meas. Charact.* **12**, 634–640 (2018)
- T. Jamali, H.K. Maleh, M.A. Khalilzadeh, *LWT-Food Sci. Technol.* **57**(2), 679–685 (2014)
- A. Baghizadeh, H.K. Maleh, Z. Khoshnama, A. Hassankhani, M. Abbasghorbani, *Food Anal. Methods* **8**, 549–557 (2015)
- S. Cheraghi, M.A. Taher, H.K. Maleh, *J. Food Compos. Anal.* **62**, 254–259 (2017)
- H.K. Maleha, K. Cellat, K. Arkan, A. Savk, F. Karimi, F. Şen, *Mater. Chem. Phys.* **250**, 123042 (2020)
- J.G. Manjunatha, M. Deraman, N.H. Basri, N.S.M. Nor, I.A. Talib, N. Ataollahi, *C.R. Chim.* **17**(5), 465–476 (2014)
- H.K. Maleh, F. Karimi, M. Alizadeh, A.L. Sanati, *Chem. Rec.* **20**, 1–12 (2020)
- H.K. Maleha, F. Karimi, S.M. Mohammadi, N. Zakariae, R. Esmaili, S. Rostamni et al., *J. Mol. Liq.* **310**, 113185 (2020)
- F.T. Javazmi, M.S. Nooshabadi, H.K. Maleh, *Talanta* **176**, 208–213 (2018)
- H.K. Maleh, A.F. Shojaei, K. Tabatabaiean, F. Karimi, R. Moradi, *Biosens. Bioelectron.* **86**, 879–884 (2016)
- M. Miraki, H.K. Maleh, M.A. Taher, S. Cheraghi, F. Karimi, S. Agarwal, V.K. Gupta, *J. Mol. Liq.* **278**, 672–676 (2019)
- H.K. Maleh, M. Sheikhsheoae, I. Sheikhsheoae, M. Ranjbar, J. Alizadeh, N.W. Maxakatob, A. Abbaspourrad, *New J Chem.* **43**, 2362–2367 (2019)
- Z. Xiaohong, Z. Zhidong, L. Xiongwei, L. Jian, H. Guohua, *Food Meas.* **11**, 548 (2016)
- A. Khodadadi, E.F. Mirzaei, H.K. Maleh, A. Abbaspourrad, V.K. Gupta, *Sens. Actuators B* **284**, 568–574 (2019)
- Q. Xu, M.L. Xie, X. Gang, Y. Hua, Z.R. Song, *Asian J. Chem.* **27**(4), 1223–1226 (2015)
- J.G. Manjunatha, *JFDA.* **26**(1), 292–299 (2018)
- E.S. Gomes, F.R.F. Leite, B.R.L. Ferraz, H.A.J.L. Mourao, A.R. Malagutti, *J. Pharm. Anal.* **9**(5), 347–357 (2019)
- S.M. Chen, M.I. Liu, S.A. Kumar, *Electroanalysis* **19**(9), 999–1007 (2007)
- J.G. Manjunatha, M. Deraman, N.H. Basri, I.A. Talib, *Arab. J. Chem.* **11**(2), 149–158 (2018)
- M.M. Charithra, J.G. Manjunatha, *J. Electrochem. Sci. Eng.* **10**(1), 29–40 (2020)
- N. Ramalakshmi, S. Muthukumar, B. Marichamy, *Ijcps.* **2**(4), 16–24 (2013)
- D.S. Nayak, N.P. Shetti, *J. Anal. Sci. Technol.* **12**(7), 1–8 (2016)
- M.M. Rahman, I.C. Jeon, *J. Braz. Chem. Soc.* **18**(6), 4100–4114 (2007)
- G. Hui, Y. Ying, *Trans. ASABE* **60**(5), 1439–1443 (2017)
- E. Sevcan, Y. Zehra, *Rev. Roum. Chim.* **63**(11), 977–986 (2018)
- Z.H. Khan, X. Liu, Y. Tang, J. Zhu, W. Hu, X. Liu, *Microchim. Acta.* **2–10** (2018)
- R. Singh, D. Rathore, C.M. Pandey, Geetanjali, R. Srivastava, *Anal. Chem. Lett.* **8**, 653–664 (2018)
- S.S. Khaloo, *Int. J. Food Prop.* **19**(10), 2272–2283 (2016)
- N. Hareesha, J.G. Manjunatha, *J. Iran Chem Soc.* (2020)
- M. Eldefrawy, E.G. Arafa Gomaa, S. Salem, F.A. Razik, *Prog. Chem. Biochem. Res.* **1**(1), 11–18 (2018)
- A. Muhammad, N.A. Yusof, R. Hajian, J. Abdullah, *J. Sens.* **16**(1), 2–13 (2016)
- S.D. Bukkitgar, N.P. Shetti, R.M. Kulkarni, *Sens. Actuator B* **255**, 1462–1470 (2018)
- F. Karimian, G.H. Rounaghi, M. Mohadeszadeh, *J. Anal. Chem.* **71**, 1057–1062 (2016)
- N.P. Shetti, S.J. Malode, S.T. Nandibewoor, *Bioelectrochemistry* **88**, 76–83 (2012)
- J.G. Manjunatha, *Sens. Biosens. Res.* **16**, 79–84 (2017)
- B.M. Amrutha, J.G. Manjunatha, A.S. Bhatt, C. Raril, P.A. Pushpanjali, *Phys. Chem. Res.* **7**(3), 523–533 (2019)
- H. Beitollahi, I. Sheikhsheoae, *Int. J. Electrochem. Sci.* **7**, 7684–7698 (2012)
- H. Guohua, L. Hongyang, J. Zhiming, Z. Danhua, W. Haifang, *Biosens. Bioelectron.* **97**, 184–195 (2017)
- R. Sriramprabha, M. Divagar, N. Ponpandian, C. Viswanathan, *J. Electrochem. Soc.* **165**, B498–B507 (2018)
- A. Sangili, P. Veerakumar, S.M. Chen, C. Rajkumar, K.C. Lin, *Microchim. Acta.* **186**, 1–12 (2019)
- A.A. Ensafi, H.E. Bafrooei, M. Amini, *Biosens. Bioelectron.* **31**, 376–381 (2012)
- S.C. Avendan, G.A. Angeles, M.T.R. Silva, G.R. Pina, M.R. Romo, M.P. Pardave, *J. Electroanal. Chem.* **609**, 17–26 (2007)
- G.S. Garbellini, R.C. Rocha-Filho, O. Fatibello-Filho, *Anal. Methods* **7**(8), 3411–3418 (2015)
- P.A. Pushpanjali, J.G. Manjunatha, M.T. Shreenivas, *Chem. Select.* **4**, 13427–13433 (2019)
- C. Raril, J.G. Manjunatha, *Microchem. J.* **154**, 104575 (2019)
- B.M. Amrutha, J.G. Manjunatha, S. AartiBhatt, N. Hareesha, *J. Mater. Environ. Sci.* **10**, 784 (2019)
- R.N. Hegde, N.P. Shetti, S.T. Nandibewoor, *Talanta* **79**, 361–368 (2009)

Publisher's Note Springer Nature remains neutral with regard to jurisdictional claims in published maps and institutional affiliations.